OBJECT BASED FOREST STAND DENSITY ESTIMATION FROM VERY HIGH RESOLUTION OPTICAL IMAGERY USING WAVELET BASED TEXTURE MEASURES

Lieven P.C. Verbeke, Frieke M.B. Van Coillie and Robert R. De Wulf

Laboratory of Forest Management and spatial Information Techniques
Department of Forest and Water Management, Faculty of Bio-science Engineering, Ghent University
Coupure Links 653, 9000 Ghent, Belgium
Lieven.Verbeke@UGent.be, Frieke.Vancoillie@UGent.be, Robert.Dewulf@UGent.be
http://dfwm.ugent.be/forman

KEY WORDS: segmentation, stand density, forest inventory, wavelets, very high resolution

ABSTRACT:

Stand density or tree density, expressed as the number of trees per unit area, is an important forest management parameter. It is used by foresters to evaluate regeneration, to assess the effect of forest management measures or as an indicator variable for other stand parameters like age, basal area and volume. A stand density estimation technique, based on the application of wavelet analysis, is presented in this work. First, very high resolution imagery is segmented using a wavelet based segmentation algorithm. Then, wavelet coefficient statistics are calculated for each separate object in order to characterize local texture. Next, the wavelet statistics are related to stand density using an artificial neural network. The established relation is finally used to produce semi-continuous stand density maps. In order to test the proposed method, several color-infrared aerial photographs (scale 1:5000) were scanned, mosaiced and converted to 25cm resolution orthophotos. A large number of trees (45,000) were manually digitized on this dataset. The available imagery was degraded to 1m and 2m spatial resolutions, and the new algorithm was applied. To put the presented method in perspective, a comparison was made with the local maximum filter, a conventional density estimation and individual tree identification method. Analysis of variance revealed that the wavelet based technique performed significantly better ($p < 0.001$) when compared with the local maximum based method, in terms of correlation, root mean square error and mean absolute difference, regardless of resolution or spectral band.

1 INTRODUCTION

Stand density or tree density, expressed as the number of trees per unit area, is an important forest management parameter. Together with other forest structure parameters like crown closure and crown diameter, it is used by foresters to evaluate regeneration (Quackenbush et al., 2000), to assess the effect of forest management measures or as an indicator variable for other stand parameters like age, basal area and volume. Most often it is assessed in large scale forest inventories, together with a large group of other tree, stand and forest variables. Given the cost (in terms of human resources and time) of field excursions, remote sensing is regarded an attractive tool for automating, facilitating or enhancing forest inventories, allowing for more timely and cost effective inventories, as is comprehensively discussed by Wulder (1998) and Boyd and Danson (2005).

A number of image processing techniques, developed to estimate stand density or locate individual trees from remotely sensed imagery, have emerged in the last decades. These techniques operate on a variety of data types and forests. Typical examples are local maximum filtering (Bolduc et al., 1999; Wulder et al., 2000, 2002, 2004; Nelson et al., 2005), valley following (Gougeon, 1995), kNN simultaneous estimation of different inventory parameters (Hömstrom, 2002), tree template matching (Quackenbush et al., 2000), local variogram modeling (St-Onge and Cavayas, 1995, 1997) or inversion of reflectance or radiative transfer models (Scarth and Stuart, 2000; Kimes et al., 2002).

Forests in Flanders, Belgium, are typically small and heterogeneous in age and species composition. Consequently, techniques for estimating forest inventory parameters like stand density, crown cover fraction or average crown diameter should be applicable in a local neighborhood. This in turn implies the use of very high resolution imagery, especially because forest patches in Flanders can be very small. According to the forest definition used by the Flemish Forest Management, the minimal area covered with trees that is considered forest can be as small as 0.5 hectares. It seems natural to use image objects, representing locally homogeneous areas, as basic inputs for any stand density estimation algorithm. Objects will typically correspond to areas smaller then actual management units, leading to stands containing several objects. Normally, tree density is regarded as a stand attribute. Even though it is impossible to provide a spatially continuous estimation of tree density, the use of objects smaller than stands allows for a semi-continuous estimation, integrating density only over a small area. Existing techniques for stand density estimation are largely based on the identification of individual trees, for which sub-meter (tens of centimeters) spatial resolution imagery is required. Such imagery is, as for now, not available from spaceborne platforms, even though the panchromatic bands of the IKONOS (1m) and QuickBird (70cm) sensors are close to meeting this requirement. Typically, sub-meter imagery will be acquired in aerial campaigns, with the associated logistic and economical issues. An alternative technique, based on the application of wavelet analysis, is presented in this work. Stand density is no longer based on individual tree identification, but is based on small-area statistics characterizing local texture. Statistics are derived from imagery with spatial resolutions higher than or equal to 1m using wavelet analysis.

2 WAVELETS

We first introduce the wavelet transform because multiple parts of the method presented here are based on this technique. Wavelet analysis is related to Fourier analysis in a sense that a signal (the image) is decomposed using a series of basis functions. As opposed to Fourier analysis, these functions are no longer stationary sine and cosine functions with different periods, but are trans-

lated, dilated and scaled versions of a localized function called a *wavelet*. The main advantage of wavelet analysis over Fourier analysis is its local support in both the space and frequency domains, whereas Fourier basis functions are local in frequency but have only global support in the space domain. A wavelet ψ is a function of zero average, which is dilated with a scale parameter s, and translated by u (Mallat, 1999):

$$\psi_{u,s}(t) = \frac{1}{\sqrt{s}}\psi\left(\frac{t-u}{s}\right) \tag{1}$$

The wavelet transform of a function f at the scale s and position u is then computed by correlating f with a wavelet (Mallat, 1999):

$$Wf(u,s) = \int_{-\infty}^{+\infty} f(t)\frac{1}{\sqrt{s}}\psi^*\left(\frac{t-u}{s}\right)dt \tag{2}$$

Equation 2 is referred to as the continuous wavelet transform (CWT), as a transform can be calculated for every possible real value of s and u. There exist a large number of wavelet functions. In this work, we have focussed on the well known Daubechies wavelet family (Daubechies, 2004). Wavelet analysis with this family of wavelets is easily implemented in filter banks. Mallat (1999) presents a fast discrete wavelet transform (DWT) that operates on finite discrete signals. In the algorithm, a discrete signal is decomposed in a lower scale *approximation* A and *detail signal* D. This is achieved by performing a discrete convolution of a low (h) and a high pass filter (g) with the original signal, combined with a binary subsampling. Both low and the high pass filter can be derived from the mother wavelet (Mallat, 1999). The decomposition formulae (with A_0 the original signal) are then (Pu and Gong, 2004; Mallat, 1999):

$$A_1[k] = \sum_{n=-\infty}^{+\infty} h[n-2k]A_0[n] \tag{3}$$

$$D_1[k] = \sum_{n=-\infty}^{+\infty} g[n-2k]A_0[n] \tag{4}$$

By iteratively applying equations 3 and 4 to consecutive approximations, starting with A_0, the original signal, the signal is decomposed in approximation and detail coefficients at scale levels 2,4,8,16,... It can be shown that such a decomposition allows for a perfect reconstruction of the original signal and constitutes an efficient (in terms of data storage) representation of the signal's detail on different scales (Mallat, 1999). The one-dimensional decomposition is easily extended to the two-dimensional case. First formulae 3 and 4 are applied to the rows of an image, yielding a set of approximation and detail coefficients. By applying the same equations to the columns of these first approximations and details, four new images are obtained, a single approximation image and a horizontal, vertical and diagonal detail image. For a more comprehensive discussion of wavelets and their applications, the reader is referred to the works of e.g. Daubechies (2004), Mallat (1999) or Goswami and Chan (1999). A number of authors have employed wavelets within a remote sensing context. For example (Pu and Gong, 2004) used wavelets for estimating LAI and crown closure mapping estimation from hyperspectral data. Ranchin and Wald (2000) and Park and Kang (2004) used wavelets for multiresolution image fusion. Noise (stripe) (Chen et al., 2006) and speckle (Sgrenzaroli et al., 2004) removal are other typical examples of the use of wavelets. An application that is especially relevant for this work is the use of detail coefficients and derived statistics as measures of local texture (Li, 2004; Simard et al., 2000; Dekker, 2003).

3 MATERIALS

3.1 Image data

For this study, 7 color infrared aerial photographs taken in October 1987 over Oud-Heverlee, Belgium were scanned and converted to an orthophoto mosaic with a spatial resolution of 20cm. A very high resolution DEM together with camera calibration data were used in this process. Note that no surface model was available; consequently some distortions (trees leaning away from the center of the photographs) could not be removed. The fact that the imagery used is of considerable age is of no importance for this study. Most important is that individual trees can be identified in the dataset. Once the very high resolution dataset was created, two degraded datasets were created with spatial resolutions of respectively 1m and 2m. Originally, we intended to apply the proposed method to IKONOS imagery. Unfortunately, the image preprocessing performed by the image supplier introduced a systematic noise that was imposable to remove. This noise is especially visible in the wavelet detail images, and therefor no evaluation of the method on IKONOS imagery was performed. It is expected though that the 1m degraded image will produce results very similar to the results that would be obtained using IKONOS imagery.

3.2 Reference data

Once the 20cm resolution mosaic was created, 104 homogeneous polygons were delineated, and within these 104 polygons, 45,000 treetops were digitized by an operator. The 104 polygons are assumed to represent homogeneous stands in terms of species composition, age and stand density (trees/ha). Both conifer and broadleaf stands are represented in this reference dataset. No broadleaf tree loans were digitized. the stand density in the reference polygons ranges from 194 to 1968 trees/ha. The distribution of the reference densities is given in figure 1. It can be seen that not all densities are represented evenly in the reference dataset. This might cause a decline in performance of the method presented for very high stand densities.

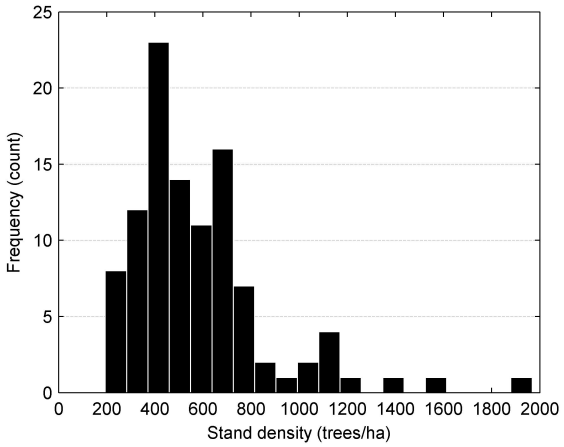

Figure 1: The distribution of the reference stand densities

4 STAND DENSITY ESTIMATION

A schematic overview of the applied method is given in figure 2. Six major steps can be discerned: (1) wavelet decomposition, (2) wavelet based segmentation, (3) calculation of per-segment wavelet statistics, (4) neural network training, (5) stand density prediction and (6) accuracy assessment. Note that it is necessary to collect reference data in the form of tree locations or small-plot densities in order to apply the proposed method. The six steps of the method presented here are discussed in more detail below.

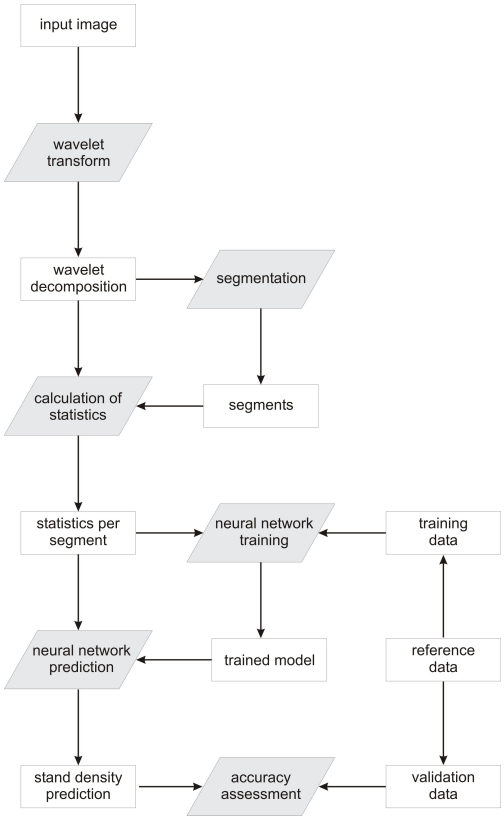

Figure 2: A schematic overview of the applied method

4.1 Wavelet decomposition

The input image is decomposed into detail and approximation images using formulas 3 and 4. The filter coefficients that are required in 3 and 4 were retrieved from literature (Mallat, 1999). As mentioned before, we use the Daubechies wavelet family, and preliminary experiments showed that good result can be obtained with the *Daubechies 4* wavelet. A four level decomposition was performed, yielding details and approximations with spatial resolutions of 2,4,8 and 16m.

4.2 Wavelet based segmentation

The wavelet based segmentation approach applied here is described in full detail in Van Coillie et al. (2006). The method is based on the use of wavelet based statistics (mean absolute value and variance) that are used to characterize local texture. The segmentation method was developed to distinguish between areas that have similar spectral characteristics, but have different textural properties because of different crown shapes, stand densities, crown closures, ...

4.3 Calculation of per-segment statistics

For every segment found in the previous step, the mean absolute value and variance of the wavelet coefficients are retrieved from the wavelet decomposition. In total, every segment is characterized by 4 scales x (3 details + 1 approximation) x 2 (mean absolute value and variance) = 32 variables. Note that we only used the most elementary statistics, and that a number of other statistics can be derived from wavelet coefficients to characterize local texture. For example (Dekker, 2003) lists additional so-called *histogram measures* like entropy and energy. Next to the calculation of the statistics for all segments, the segments are intersected with the manually digitized reference polygons. In these polygons, an operator digitized every single treetop. First all intersected segments with an area smaller than $500m^2$ are eliminated. Then the trees present in the other segments are counted and the wavelet statistics are retrieved from the wavelet decomposition yielding a reference dataset that will be used to train an artificial neural network, and to assess the accuracy of the established relationship between wavelet coefficients and stand density.

4.4 Neural network training

Once the wavelet statistics have been calculated, they have to be related to the target stand (segment) density. The reference dataset is split up in a training and a validation dataset. For each segment in the training set, the mean absolute value and the variance of the wavelet coefficients is used in combination with the target stand density to train an artificial neural network (ANN). ANNs are powerful, distribution-free models that can be trained to map *a priori* unknown input-output relationships. They are especially appreciated because of their generalisation capabilities, i.e. the ability to correctly process previously unseen data. We will not elaborate on ANN models; the reader is referred to the works of e.g. Haykin (1999) or Bishop (1997) for a comprehensive discussion on neural networks. We used feed-forward neural networks trained with the well known back-propagation algorithm, with momentum parameter. The number of input neurons in the network corresponds the the total number of available wavelet statistics, in this case 32 (four scales times four coefficients times two statistics). We used ten hidden neurons, a number determined in a trial and error process. A single output neuron is used, as stand density is the only target variable. The target variable was rescaled and transformed logarithmically to map the target density onto the interval $[0, 1]$, the output range of the sigmoid activation functions of the network neurons. Each neural network is trained until the point of maximal generalization, i.e. the training cycle for which the error calculated on the validation set is minimal. After training, the validation set is processed by the network, allowing for the accuracy assessment of the predicted stand densities.

4.5 Neural network prediction

A trained network can now be used to produce stand density estimates for all segments in the image. Therefor the dataset containing the 32 wavelet based statistics for each segment is fed to the trained neural network. The predicted values are then transformed back to stand densities, that can be used to produce a semi-continuous stand density map, that is masked with a manually digitized polygon containing only the forested area.

4.6 Accuracy assessment

In order to test the accuracy of the predicted stand density, a number of error measures were calculated by comparing the predicted stand density with a validation dataset. The error measures used

here are correlation ρ, root mean square error (RMSE) and mean absolute error (MAE). RMSE and MAE are respectively calculated as follows:

$$RMSE = \sqrt{\frac{\sum_{s=1}^{n}(prediction_s - target_s)^2}{n}} \quad (5)$$

$$MAE = \frac{\sum_{s=1}^{n}|prediction_s - target_s|}{n} \quad (6)$$

with n the number of segments in the validation set. To put the new method in perspective, it is compared with results obtained with the well known local maximum filter (Bolduc et al., 1999; Wulder et al., 2000, 2002, 2004; Nelson et al., 2005). The local maximum filter assumes that tree tops are the brightest part of a tree, and that individual tree tops can be identified by investigating if the central pixel of a moving window contains the maximum reflectance value (or digital number in this case) in this window. Once all local maxima are identified, it is possible to count the number of maxima in each segment, leading to estimates of the number of trees per area unit in each separate segment. In the ideal case, it is possible to identify individual trees, and the number of maxima will correspond with the number of trees in each segments. Because of a number of reasons (spatial resolution, irregular crown shapes, ...) this most certainly will not be the case. Therefore, as with the method presented, the reference data was split up in 10 pairs of training and validation datasets. The training data was used to construct a linear relationship between the number of local maxima and the target stand density. Afterwards, this linear relationship was used to predict the stand density for the segments in the validation dataset. The error measures mentioned above were than calculated for each validation set.

5 RESULTS AND DISCUSSION

The new method presented in this paper was evaluated on the red and near-infrared band of the 1m and 2m spatial resolution version of the very high resolution reference image. The wavelet-ANN and the local maximum based methods were tested by splitting up the available reference dataset into a training set containing 60% of the reference data and a test set containing 40% of the data. This splitting up in mutual exclusive training and test sets was repeated 5 times for the wavelet-ANN method and 10 times for the local maximum based method (with window sizes 3 and 5 for the 1m resolution image, and 3 for the 2m resolution image). Repetitions were necessary because neural networks are initialized randomly, and network initialization is known to influence the final performance of the network. Also, because tree stand densities are not evenly distributed over the entire interval of possible densities (figure 1, it is possible that the final performance of the methods under study depends on the segments present in the training dataset. The difference between the number of replications between the wavelet-ANN method and the local maximum method was due to practical issues.

First the images were segmented. Then the segments were intersected with the available reference polygons. All segments with an area smaller than 500m were removed, because it is assumed that (especially for the lower resolution wavelet coefficients) statistics can not be reliably estimated when only few pixels are present inside a segment. Wavelet statistics were collected for the remaining segments. The reference dataset constructed was split up in a number of mutual exclusive training and validation datasets, as explained above.

	band	technique	ρ	RMSE	MAE
1m	red	lm ws 3	0.62	179.30	134.31
		lm ws 5	0.64	174.69	128.71
		wavelet	0.80	158.00	105.46
	nir	lm ws 3	0.64	175.42	132.31
		lm ws 5	0.56	189.45	141.24
		wavelet	0.85	134.60	100.58
2m	red	lm ws 3	0.16	238.90	173.64
		wavelet	0.56	175.35	135.00
	nir	lm ws 3	0.19	235.23	172.24
		wavelet	0.55	184.91	142.19

Table 1: Comparison of the wavelet-ANN technique with the local maximum filter in terms of correlation (ρ), root mean square error (RMSE) and mean absolute error (MAE) for two spatial resolutions and two spectral bands

Both the wavelet-ANN and the local maximum based methods were applied to all of the training sets, and the accuracy measures described in section 4.6 were calculated. The average performance for the three accuracy measures is displayed in table 1. It can be seen in the table that the wavelet-ANN technique outperforms local maximum estimation of stand density regardless of the accuracy measure used. Performing an analysis of variance on the 1m results revealed that these differences are also statistical significant ($p < 0.001$). As expected, using the lower resolution image yielded lower performance for all methods, but differences were still statistically significant ($p < 0.001$). No statistical difference (at the 95% level) between the results obtained with different spectral bands could be detected. The difference between the performance of the wavelet-ANN technique and the local maximum based estimation of density is very likely due to the spatial resolution of the images used. Indeed, for the local maximum method to perform well, it is necessary to be able to identify individual trees, a condition not always fulfilled, especially for stands with high densities. It should be noted that even though the wavelet-ANN technique performs significantly better on the 2m resolution image, the results are poor, and probably not very useful. It seems that a 1m resolution is necessary in order to provide reliably estimates of stand density. An example of the obtained relation between validation data predictions and target data is given in figure 3. It can be seen that the relation between estimates and reference data is very close to the ideal case. Ideally the slope of 0.947 should be 1.0, and the bias of 36.3 should be zero. This is an unexpectedly good result, as a number of different tree species (broadleaf and coniferous) are present in the study area.

Finally, after the relation between wavelet-based statistics and stand density was established, it was possible to process all segments in order to produce a semi-continuous stand density map. The result of such a map if given in figure 4. The individual segments in the image appear somewhat coarse, a consequence of the segmentation technique that was based on multi-level wavelet coefficients with decreasing spatial resolution. The resulting map is expected to have an accuracy very close to the accuracy of the validation data results. Still additional errors are introduced in the density map. The proportion of broadleaf stands present in the image was larger than the proportion present in the reference dataset. Consequently, broadleaf stands are under sampled, and density predictions for those stands will likely be less reliable.

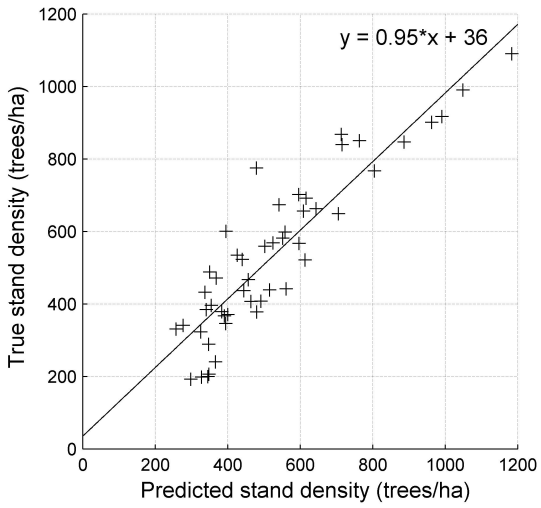

Figure 3: The relation between wavelet-ANN predicted and true stand density for one of the five cross validation cases, 1m resolution, red band

6 CONCLUSIONS AND FUTURE WORK

In this work, a new method for estimating stand density expressed as the number of trees per hectare was presented. The new method is based on the use of multi-level wavelet decomposition. First, a wavelet based segmentation was performed on color infrared images with spatial resolutions of 1m and 2m. Next, wavelet derived statistics were calculated for all segments. A relation between a number of reference segments and the wavelet-based statistics was established by training an artificial neural network. The method was evaluated by calculating three error measures, correlation, root mean square error and mean absolute error, on a number of independent validation segments. To put the new method in perspective, a comparison was made with the well known local maximum filter. It was found that the wavelet-ANN method outperformed the local maximum filter ($p < 0.001$) regardless of the resolution or spectral band used. Future work will concentrate on further evaluation of the method presented here, by testing additional spectral bands and spatial resolutions, and by comparing with other established stand density estimation methods. Also, it will be investigated whether other structural stand parameters like crown closure and crown diameter can be reliably estimated.

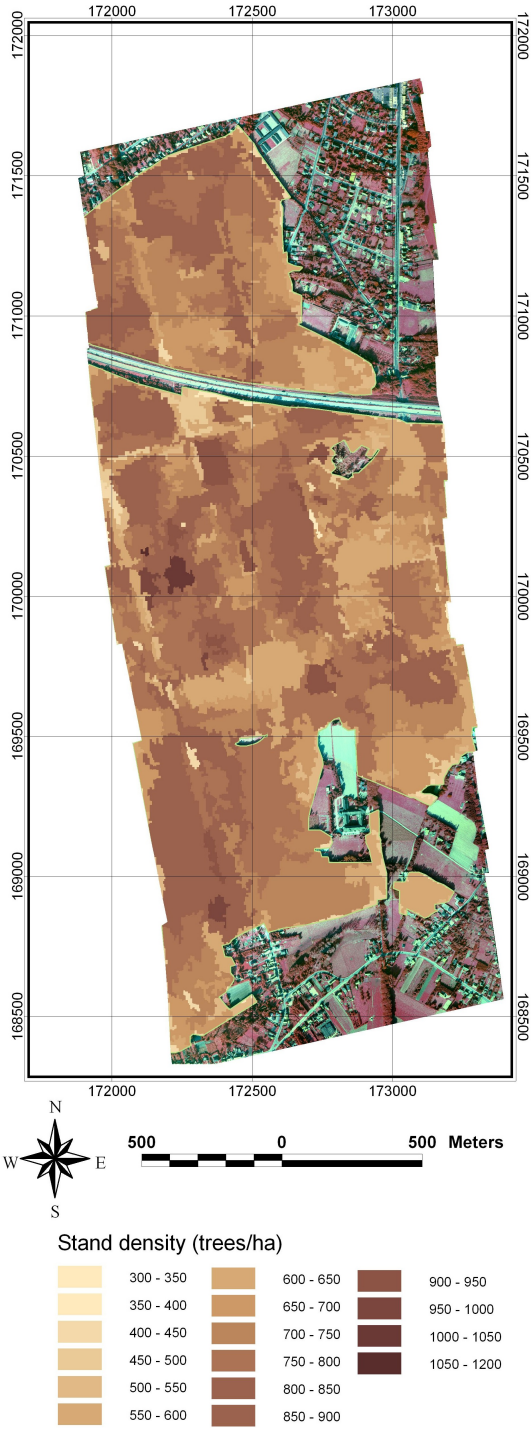

Figure 4: An example of the obtained results: 1m resolution nir band, correlation=0.88, rmse=128.71, mean absolute difference=89.63, background is a false color composite of the study area

References

Bishop, C. M., 1997. Neural Networks for Pattern Recognition. fourth edn, Clarendon Press, Oxford.

Bolduc, P., Lowell, K. and Edwards, G., 1999. Automated estimation of localized forest volumes from large-scale aerial photographs and ancillary cartographic information in a boreal forest. International Journal of Remote Sensing 20(18), pp. 3611–3624.

Boyd, D. and Danson, F., 2005. Satellite remote sensing of forest resources: three decades of research development. Progress in Physical Geography 29(1), pp. 1–26.

Chen, J. S., Lin, H., Shao, Y. and Yang, L. M., 2006. Oblique striping removal in remote sensing imagery based on wavelet transform. International Journal of Remote Sensing 27(8), pp. 1717–1723.

Daubechies, I., 2004. Ten lectures on wavelets. CBMS-NSF Regional Conference Series in Applied Mathematics. Vol. 61, Society for Industrial and Applied Mathematics, Philadelphia.

Dekker, R. J., 2003. Texture analysis and classification of ers sar images for map updating of urban areas in the netherlands. IEEE Transactions on Geoscience and Remote Sensing 41(9), pp. 1950–1958.

Goswami, J. and Chan, A., 1999. Fundamentals of wavelets. Theory, algorithms and applications. John Wiley & Sons, New York.

Gougeon, F., 1995. A crown-following approach to the automatic delineation of individual tree crowns in high spatial resolution aerial images. Canadian Journal of Remote Sensing 21, pp. 274–284.

Haykin, S., 1999. Neural Networks: A Comprehensive Foundation. Prentice Hall, New Jersey.

Hömstrom, H., 2002. Estimation of single-tree characteristics using the kn method and plotwise aerial photograph interpretations. Forest Ecology and Management 167, pp. 303–314.

Kimes, D., Gastelly-Etchegorry, J. and Estve, P., 2002. Recovery of forest canopy characteristics through inversion of a complex 3d model. Remote Sensing of Environment 79, pp. 320–328.

Li, J., 2004. Wavelet-based feature extraction for improved endmember abundance estimation in linear unmixing of hyperspectral signals. IEEE Transactions on Geoscience and Remote Sensing 42(3), pp. 644–649.

Mallat, S., 1999. A wavelet tour of signal processing. Academic Press, London.

Nelson, T., Boots, B. and Wulder, A., 2005. Techniques for accuracy assessment of tree locations extracted from remotely sensed imagery. Journal of Environmental Management 74, pp. 265–271.

Park, J. H. and Kang, M. G., 2004. Spatially adaptive multiresolution multispectral image fusion. International Journal of Remote Sensing 25(23), pp. 5491–5508.

Pu, R. L. and Gong, P., 2004. Wavelet transform applied to eo-1 hyperspectral data for forest lai and crown closure mapping. Remote Sensing of Environment 91(2), pp. 212–224.

Quackenbush, L., Hopkins, P. and Kinn, G., 2000. Developing forestry products from high resolution digital aerial imagery. Photogrammetric Engineering and Remote Sensing 66(11), pp. 1337–1346.

Ranchin, T. and Wald, L., 2000. Fusion of high spatial and spectral resolution images: The ARSIS concept and its implementation. Photogrammetric Engineering and Remote Sensing 66, pp. 49–61.

Scarth, P. and Stuart, P., 2000. Determining forest structural attributes using an inverted geometric-optical model in mixed eucalypt forests, southeast queensland, australia. Remote Sensing of Environment 71, pp. 141–157.

Sgrenzaroli, M., Baraldi, A., De Grandi, G. D., Eva, H. and Achard, F., 2004. A novel approach to the classification of regional-scale radar mosaics for tropical vegetation mapping. IEEE Transactions on Geoscience and Remote Sensing 42(11), pp. 2654–2669.

Simard, M., Saatchi, S. S. and De Grandi, G., 2000. The use of decision tree and multiscale texture for classification of jers-1 sar data over tropical forest. IEEE Transactions on Geoscience and Remote Sensing 38(5), pp. 2310–2321.

St-Onge, B. and Cavayas, F., 1995. Estimation forest stand structure from high resolution imagery using the directional variogram. International Journal of Remote Sensing 16(11), pp. 1999–2021.

St-Onge, B. and Cavayas, F., 1997. Automated forest structure mapping from high resolution imagery based on directional semivariogram estimates. Remote Sensing of Environment 61, pp. 82–95.

Van Coillie, F. M. B., Verbeke, L. P. C. and De Wulf, R. R., 2006. Semi-automated forest stand delineation using wavelet-based segmentation of very high resolution optical imagery in flanders, belgium. In: 1st International Conference on Object-based Image Analysis (OBIA 2006).

Wulder, M., 1998. Optical remote sensing techniques for the assessment of forest inventory and biophysical parameters. Progress in Physical Geography 22(4), pp. 449–476.

Wulder, M., Niemann, K. and Goodenough, D., 2000. Local maximum filtering for the extraction of tree locations and basal area from high spatial resolution imagery. Remote Sensing of Environment 73, pp. 103–114.

Wulder, M., Niemann, K. and Goodenough, D., 2002. Error reduction methods for local maximum filtering of high spatial resolution imagery for locating trees. Canadian Journal of Remote Sensing 28(5), pp. 621–628.

Wulder, M., White, J., Niemann, K. and Nelson, T., 2004. Comparison of airborne and satellite high spatial resolution data for the identification of individual trees with local maxima filtering. International Journal of Remote Sensing 25(11), pp. 2225–2232.